Photocatalytic Formic Acid Conversion on CdS Nanocrystals with Controllable Selectivity for H₂ or CO

Moritz F. Kuehnel,‡ David W. Wakerley,‡ Katherine L. Orchard, and Erwin Reisner*[a]

Abstract: Formic acid is considered a promising energy carrier and hydrogen storage material for a carbon-neutral economy. We present an inexpensive system for the selective room temperature photocatalytic conversion of formic acid to either hydrogen or carbon monoxide. Under visible-light irradiation (λ>420 nm, 1 sun), suspensions of ligand-capped cadmium sulfide nanocrystals in formic acid/sodium formate release up to 116±14 mmol H_2 g_{cat}^{-1} h^{-1} with >99% selectivity when combined with a cobalt co-catalyst; the quantum yield at λ=460 nm was 21.5±2.7%. In the absence of capping ligands, suspensions of the same photocatalyst in aqueous sodium formate generate up to 102±13 mmol CO g_{cat}^{-1} h^{-1} with >95% selectivity and 19.7±2.7% quantum yield. H_2 and CO production was sustained for more than one week with turnover numbers greater than $6\cdot10^5$ and $3\cdot10^6$, respectively.

The replacement of conventional fossil fuels with a CO_2-neutral energy cycle is a key global challenge for developing a sustainable economy. Hydrogen holds promise as a secondary energy vector for use in fuel cells but its safe storage and transport remain the subject of intense research.[1] Formic acid (HCO_2H, FA) has received considerable attention as a potential renewable fuel of high energy density. Its low toxicity and high gravimetric hydrogen content of 4.4% render FA a promising hydrogen storage material with CO_2 as the only by-product of H_2 release.[2] CO_2 recycling *via* mild homogeneous CO_2 hydrogenation to FA has become a feasible process to store H_2 derived from renewable sources.[3] In addition, a growing number of synthetic catalysts[4] and enzymes[5] promote storage of electrical energy by electrochemical reduction of CO_2 to FA. FA is also a major product of biomass processing.[6]

Although FA dehydrogenation (FA-to-H_2) is an exergonic process (Scheme 1), efficient liberation of H_2 requires additional energy input (*i.e.*, high temperatures or light) unless precious metal-based catalysts are employed.[7],[8] The high cost and low abundance of these catalysts, however, precludes scalability and thus a widespread application. Precious metal-free alternatives typically require elevated temperatures and organic solvents, limiting their potential use in portable applications and decreasing their overall energy density.[9] Only recently, photochemical decomposition of FA has attracted increasing interest as an alternative approach to generate H_2 from FA at

room temperature. Photocatalysts based on Pd,[10] AuPd,[11] Pt,[12] Rh[13], and Ru[14] have demonstrated activities up to 154 mmol H_2 g_{cat}^{-1} h^{-1}. Examples of precious metal-free catalysts are scarce and show substantially lower activity.[15]

$$HCO_2H \begin{cases} \xrightarrow{\text{dehydrogenation}} H_2 + CO_2 & \Delta G^0 = -48.8 \text{ kJ mol}^{-1} \quad (1) \\ \xrightarrow{\text{dehydration}} CO + H_2O & \Delta G^0 = -28.5 \text{ kJ mol}^{-1} \quad (2) \end{cases}$$

Scheme 1. Thermodynamics of formic acid decomposition pathways.[16]

Despite the pivotal role of nano-crystalline semiconductors (commonly referred to as quantum dots, QDs)[17] in photovoltaics[18] and artificial photosynthesis,[19] little is known about their activity towards photochemical FA-to-H_2 conversion. Cadmium sulfide is among the most studied QD materials owing to its ease of preparation, low cost and high absorption of visible light. Whereas bulk CdS powder shows limited photocatalytic FA-to-H_2 activity,[20] enhanced activity has been achieved by confinement on a titanate nanotube support,[21] by construction of CdS-ZnS heterojunctions[22] or by introduction of precious metal co-catalysts such as Pt[21a, 23] and Ru.[22, 24] A precious-metal free hybrid system comprised of CdS and a H_2 producing enzyme (hydrogenase) exhibited low selectivity and suffered from enzyme inhibition.[25] Moreover, none of these systems show flexibility with respect to the reaction products.

FA is known to undergo two pathways of decomposition, to give either H_2 or carbon monoxide (Scheme 1). CO is a valuable synthon in the chemical industry and synthesis gas, a mixture of CO and H_2, can be used to generate liquid fuels such as methanol and hydrocarbons *via* the Fischer-Tropsch process.[26] CO is currently produced from fossil sources, but despite its critical importance, the sustainable generation of CO from FA has received little attention and no chemical CO storage process is currently available.[27] FA contains more than 60 wt% CO, which can be released upon treatment with excess dehydrating agents such as conc. H_2SO_4, but catalytic FA-to-CO conversion typically requires high temperatures.[28] Consequently, selective photocatalytic FA-to-CO has not been reported. This work presents an inexpensive and highly active CdS-based photocatalyst that efficiently uses FA as a clean storage material for the controlled generation of either H_2 or CO under ambient conditions.

Monodisperse CdS nanocrystals with 3-mercaptopropionic acid (MPA) capping ligands (QD-MPA) were prepared according to literature procedures from oleic acid capped CdS nanoparticles by basic ligand exchange (λ_{max} = 443 nm, D = 4.4±0.4 nm, Fig. S1).[19c, 29] Under simulated solar light irradiation (AM1.5G, 100 mW cm^{-2}, λ>420 nm, 25°C, see SI for details), dispersions of QD-MPA in 4.0 M sodium formate in FA
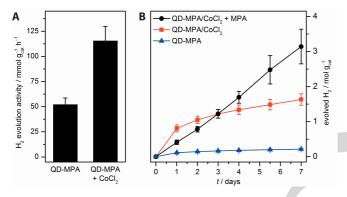
‡ These authors contributed equally.

[a] Dr. M. F. Kuehnel, D. W. Wakerley, Dr. K. L. Orchard, Dr. E. Reisner
Christian Doppler Laboratory for Sustainable SynGas Chemistry
Department of Chemistry
University of Cambridge
Lensfield Road, CB2 1EW, Cambridge, UK
E-mail: reisner@ch.cam.ac.uk
http://www-reisner.ch.cam.ac.uk

(Laboratory Reagent Grade, >90%) generated H_2 at initial rates of 52.1±6.6 mmol H_2 g_{cat}^{-1} h^{-1} (Fig. 1A, Table 1). Addition of up to 0.5 mM $CoCl_2 \cdot 6H_2O$ resulted in enhanced rates of up to 116±14 mmol H_2 g_{cat}^{-1} h^{-1} (QD:Co ratio approx. 500:1, see Fig. S2 and Tables S1-S2 for optimization details). Only traces of CO were detected in the headspace gas (670±146 ppm absolute, 0.614±0.065% with respect to H_2). When the full solar spectrum was used for irradiation, the rate increased to 218±22 mmol H_2 g_{cat}^{-1} h^{-1} (Fig. S3), showing that both the visible and UV portion of the solar spectrum are used for catalysis; light dependence of the catalyst was confirmed by varying the light intensity (Fig. S4). At λ=460 nm, the external quantum yield (EQY) was 21.2±2.7% (Table S3). The CO_2:H_2 ratio increased over time (Fig. S5) but remained below the theoretical 1:1 stoichiometry (Scheme 1), presumably due to higher solubility of CO_2 than H_2 in FA. H_2 generation even proceeds in FA without added sodium formate, albeit at a lower rate of 1.4±0.3 mmol H_2 g_{cat}^{-1} h^{-1}. No H_2 was formed in the dark or without photocatalyst (Table S2).

Figure 1. Photocatalytic FA dehydrogenation: A) Initial activity of QD-MPA with and without added co-catalyst (1 h of irradiation); B) Long-term activity of QD-MPA [100 mW cm^{-2} AM1.5G, λ>420 nm; 0.91 µM QD-MPA (176 µg mL^{-1}), 4.0 M $NaHCO_2$ in FA; $CoCl_2$ = 0.5 mM $CoCl_2 \cdot 6H_2O$, MPA = 140 mM 3-mercaptopropionic acid].

Long-term experiments were performed in order to demonstrate the stability of this system (Fig. 1B, Table S4). H_2 evolution was sustained for more than 7 days even in the absence of a co-catalyst. The H_2-evolution rate gradually decreased during the first 48 h of irradiation stabilizing at 4.4±1.3 mmol H_2 g_{cat}^{-1} h^{-1} and 0.52±0.17 mmol H_2 g_{cat}^{-1} h^{-1} with and without co-catalyst, respectively. When excess MPA (140 mM) was added to the QD-MPA/$CoCl_2$ system prior to irradiation, a lower initial rate of 18.7±2.9 mmol H_2 g_{cat}^{-1} h^{-1} was observed, but this activity remained constant over the course of one week. More than 3 mol H_2 g_{cat}^{-1} were generated after one week, which corresponds to over 600,000 turnovers per QD. Transmission electron microscopy (TEM) after photocatalysis indicated the formation of aggregates that retained nanocrystalline features (Fig. S6). Particle aggregation over time was monitored *in situ* by UV-vis spectroscopy. When QD-MPA is added to FA, a red shift of the absorption maximum indicates aggregation, which increases further during irradiation (Fig. S7A).[30] In the presence of MPA, a red shift was observed upon addition to FA, but no further change occurred during irradiation (Fig. S7B), suggesting

that MPA enhances the lifetime of QD-MPA during photocatalysis by preventing aggregation.

To the best of our knowledge, the catalytic activity and lifetime of QD-MPA/$CoCl_2$ surpasses all previously reported heterogeneous photocatalysts for FA-to-H_2 conversion at ambient conditions, including those based on precious metals (Table 1, see Table S5 for a more comprehensive comparison). The most active heterogeneous catalyst to date, a Pd-C_3N_4 nanocomposite evolves 53.4 mmol H_2 g_{cat}^{-1} h^{-1} with quantitative H_2 selectivity for up to 6 hours. Without added co-catalyst, QD-MPA shows a comparable activity, whereas QD-MPA/$CoCl_2$ is more than twice as active and shows an improved long-term stability. A Ru-based homogeneous photocatalyst was reported to achieve 154 mmol H_2 g_{cat}^{-1} h^{-1} in DMF solution, but no selectivity was reported.[14] The best precious metal-free photocatalyst, CdS-ZnS particles, can evolve up to 1.24±0.02 mmol H_2 g_{cat}^{-1} h^{-1} under visible-light irradiation (selectivity not reported),[22] more than 2 orders of magnitude less than QD-MPA/$CoCl_2$.
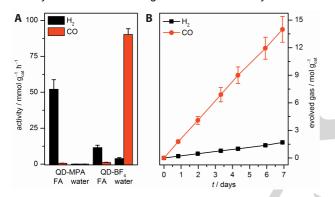
Table 1. Comparison of selected photocatalysts for visible light-driven FA-to-H_2 conversion under ambient conditions (see Table S5 for more examples).

catalyst	activity[a] [mmol H_2 g_{cat}^{-1} h^{-1}]	selectivity[b] [%]	EQY [%]	lifetime [h]	ref
Pd-C_3N_4	53.4	100	n/a	>6	[10b]
AuPd-TiO_2	17.7[c]	99.7	15.6	>9	[11b]
Pt-CdS	1.22	n/a	21.4	>30	[23a]
Ru-CdS/ZnS	5.85±0.09	n/a	20	>40	[22]
CdS/ZnS	1.24±0.02	n/a	n/a	>40	[22]
H_2ase-CdS[d]	0.356	20	3.1	>3.5	[25]
[$RuCl_2$(PhH)]$_2$ + 12 PPh$_3$	154[e]	n/a	n/a	>5	[14]
[$Fe_3(CO)_{12}$] + PPh$_3$, tpy[f]	2.7[e]	"trace CO"	n/a	>24	[15c]
QD-MPA	52.1±6.6	98.8±0.1	n/a	>168	this work
QD-MPA/ $CoCl_2$	116±14	99.4±0.1	21.2 ±2.7	>168	this work
QD-MPA/ $CoCl_2$	218±22[c]	98.9±0.1	n/a	>24	this work

[a] For an accurate comparison, published data was converted to gravimetric activity using the mass of the entire photocatalyst used in the reaction; [b] selectivity = 100% * $n$$H_2$ / ($n$$H_2$ + nCO); [c] full solar spectrum irradiation; [d] H_2ase = hydrogenase; [e] λ>380 nm; [f] tpy = 2,2':6',2''-terpyridine.

Insight into the nature of the active catalyst was sought by separating QD-MPA/$CoCl_2$ from the reaction mixture by centrifugation after 1 h photocatalysis. When the solid residue was re-dispersed in fresh reaction medium without added co-catalyst, the observed H_2 evolution activity was similar to QD-MPA in the absence of co-catalyst, suggesting that the active
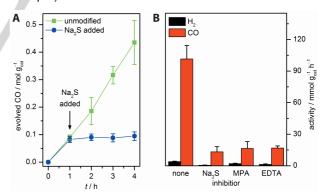
catalyst is not attached to the QDs. The QD-free supernatant did not show any activity (Fig. S8, Table S6). Inductively coupled plasma optical emission spectrometry (ICP-OES) measurements of the solid confirm the absence of Co (Co:Cd atomic ratio in solid $<(4.8\pm1.9)\times10^{-4}$:1; in contrast to 0.44:1 in the entire sample before catalysis). These findings and the absence of an induction period for H_2 evolution with QD-MPA/CoCl$_2$ lend further support to the homogeneous nature of the active co-catalyst. Cobalt species are known to function as homogeneous hydrogen evolving catalysts in the presence of nanocrystalline semiconductors.[31] Co-modification is also known to enhance electrocatalytic formate oxidation activity[32] and there is precedent for homogeneous oxidation of FA by Co^{3+} ions.[33] The mechanism of FA-to-H_2 conversion could therefore consist of formate oxidation by photo-generated holes and subsequent proton reduction by photo-excited electrons.[20, 34] In this case, either the reductive half reaction, the oxidative half reaction, or both are enhanced by Co catalysis. These possibilities are currently under further investigation in our laboratory.

Figure 2. Photocatalytic FA dehydration (100 mW cm^{-2} AM1.5G, λ>420 nm): A) Effect of solvent on the product selectivity of CdS QDs in the absence of CoCl$_2$ co-catalyst (see Table S3 for conditions); B) long term activity of QD-BF$_4$ [0.0611 µM QD-BF$_4$ (14.4 µg mL^{-1}), 4.0 M NaHCO$_2$ in 2.5 M aqueous KOH/CO$_2$ pH 9.7].

With the reactivity of nanocrystalline CdS towards formate established, we sought possibilities to tune the reaction pathway towards FA-to-CO conversion (Scheme 1, eq. 2). In aqueous formate solution, the activity of QD-MPA was much lower than in FA but showed a reversed selectivity with CO as the main decomposition product (60±7% CO, Fig. 2A, Table S2). To enhance the photocatalytic activity in aqueous solution, we studied the effect of QD surface modification. Ligand-free, charge-stabilized CdS nanocrystals of (QD-BF$_4$) were prepared from oleic acid capped CdS nanocrystals following a modified reactive ligand stripping procedure using [Me$_3$O]BF$_4$ in the presence of N,N-dimethylformamide (DMF) to remove the oleic acid capping groups.[35] Ligand stripping led to a blue-shift of the absorption maximum indicative of a decrease in QD size (Fig. S9B). This is presumably a result of etching by BF$_4^-$ anions as shown for CdTe QDs.[36] Larger QD precursors (λ_{max} = 466 nm, D = 6.0±0.9 nm) were therefore used in order to obtain QD-BF$_4$ with a diameter similar to QD-MPA (λ_{max} = 445 nm, D = 4.9±0.7 nm, Fig. S9). QD-BF$_4$ showed a drastically enhanced photocatalytic FA-to-CO activity in water compared to QD-MPA

(Fig. 2A). Under optimized conditions, up to 102±13 mmol CO g$_{cat}^{-1}$ h^{-1} are formed with 96.3±0.1% selectivity (4.0 M NaHCO$_2$ in 2.5 M KOH/CO$_2$ pH 9.7; see Fig. S10-S12 and Tables S7-S8 for optimization details). In FA solution, QD-BF$_4$ showed an FA decomposition selectivity towards H_2 that was comparable to QD-MPA, but with lower activity (Fig. 2A, Table S2). The selectivity switchover to CO is therefore not a result of ligand removal, but promoted by the basic aqueous environment. This is further corroborated by a strong pH-dependence of the product selectivity, with FA-to-H_2 becoming more pronounced in neutral and acidic solution (Fig. S10, Table S7); addition of MPA to QD-BF$_4$ in aqueous formate solution did not affect the product selectivity (*vide infra*). Effects of water on the gas-phase photocatalytic FA decomposition have been previously documented.[37]

Aqueous QD-BF$_4$ is remarkably robust and sustained CO production over the course of one week with no detectable decrease in activity; more than 14 mol CO g$_{cat}^{-1}$ were generated, which corresponds to 3,000,000 turnovers per QD (Fig. 2B, Table S9). No activity was seen in the absence of light (Table S2, entry 16; Fig. S13), confirming that irradiation provides the necessary activation energy for formate dehydration. Since irradiation of CdS generates electron/hole pairs, we propose that the reaction mechanism is centered around the charge separation by the QD. Assuming that one photon is required to generate one CO molecule, a minimum EQY of 19.7±2.7% was recorded at λ=460 nm (Table S10, see SI for further details). Formate was established as the sole source of CO using ^{13}C labelled sodium formate through IR spectroscopy (Fig. S14). TEM analysis after catalysis indicates the formation of nanostructured aggregates (Fig. S15). This was corroborated through an observed red-shift in the UV-vis spectrum (Fig. S16, *vide supra*).

Figure 3. Effects of inhibitors on the photocatalytic formate dehydration: A) In-situ inhibition of photocatalytic activity by Na$_2$S addition (111 mM); B) comparison of different inhibitors [100 mW cm^{-2} AM1.5G, λ>420 nm; 0.0611 µM QD-BF$_4$ (14.4 µg mL^{-1}), 4.0 M NaHCO$_2$, 2.5 M aqueous KOH/CO$_2$ pH 9.7; 111 mM Na$_2$S, 111 mM MPA or 83.3 mM Na$_2$EDTA].

Addition of CoCl$_2$ to QD-BF$_4$ or QD-MPA did not increase the photocatalytic activity in aqueous solution (Table S2), indicating that the CdS particle surface itself plays an essential role in the catalytic activity. Mechanistic studies were performed to further support this hypothesis (Table S11-S12). Addition of excess Na$_2$S to an active sample of QD-BF$_4$ in aqueous sodium formate

solution resulted in a sudden drop in catalytic activity (Fig. 3A), suggesting that sulfide ions block the catalytically active sites; addition of MPA showed a similar effect (Fig. 3B). At the same time, no increase in H_2 evolution was observed in either case proving that S^{2-} ions are not simply acting as electron donors and that addition of MPA has not resulted in a selectivity-switch towards H_2 production. We hypothesize that Cd ions form the active site for CO evolution. When EDTA was added in order to selectively complex surface-bound Cd^{2+}, a similar decrease in CO evolution activity was observed, providing further evidence to the crucial role of surface Cd^{2+} ions for dehydration activity. X-ray photoelectron spectra (XPS) of sulfide-poisoned $QD-BF_4$ exhibit a slight shift of the Cd(3d) peaks to lower binding energies, very similar to the spectrum of QD-MPA (Fig. S18, Table S13). In addition, a shoulder on the Cd(3d) signals is observed at lower binding energy that is absent in unmodified $QD-BF_4$. Little effect on the Cd:S stoichiometry was observed by XPS (Table S13). These data indicate that Na_2S addition leads to a distortion of the Cd environment. The resemblance of the poisoned environment to that of inactive QD-MPA suggests that the active site is Cd-based. Previous studies on thermal FA decomposition have established the importance of surface effects,[38] such as H_2O coverage[39] and surface acidity/basicity,[40] on the activity and selectivity. Further studies to clarify how a Cd-based active site alters the outcome of electron/hole transfer to promote CO rather than CO_2 formation are currently underway in our laboratory.

In summary, we have developed an inexpensive and highly active photocatalyst system for sunlight-driven conversion of formic acid with controlled selectivity and long-term stability. Ligand-capped CdS quantum dots with a cobalt co-catalyst generate H_2 with unprecedented activity and >99% selectivity when dispersed in formic acid. In contrast, CO formation is strongly favoured in aqueous solution following ligand stripping and proceeds with high activity and efficiency. With this first example of selective photocatalytic formic acid to CO conversion, we introduce formic acid as a renewable CO storage material with more than 60 wt% capacity. This work demonstrates that careful matching of engineered particle surfaces with optimized reaction media enables a novel flexibility in the sustainable use of formic acid to generate valuable chemical feedstocks.

Acknowledgements

References

[1] a) J. O. M. Bockris, *Science* **1972**, *176*, 1323; b) Q.-L. Zhu, Q. Xu, *Energy Environ. Sci.* **2015**, *8*, 478-512; c) A. F. Dalebrook, W. Gan, M. Grasemann, S. Moret, G. Laurenczy, *Chem. Commun.* **2013**, *49*, 8735-8751.

[2] a) S. Enthaler, J. von Langermann, T. Schmidt, *Energy Environ. Sci.* **2010**, *3*, 1207-1217; b) R. Williams, R. S. Crandall, A. Bloom, *Appl. Phys. Lett.* **1978**, *33*, 381-383.

[3] a) S. Moret, P. J. Dyson, G. Laurenczy, *Nat. Commun.* **2014**, *5*; b) K. Schuchmann, V. Müller, *Science* **2013**, *342*, 1382-1385; c) M. S. Jeletic, M. T. Mock, A. M. Appel, J. C. Linehan, *J. Am. Chem. Soc.* **2013**, *135*, 11533-11536; d) S. Wesselbaum, U. Hintermair, W. Leitner, *Angew. Chem. Int. Ed.* **2012**, *51*, 8585-8588; e) J. F. Hull, Y. Himeda, W.-H. Wang, B. Hashiguchi, R. Periana, D. J. Szalda, J. T. Muckerman, E. Fujita, *Nature Chem.* **2012**, *4*, 383-388; f) R. Langer, Y. Diskin-Posner, G. Leitus, L. J. W. Shimon, Y. Ben-David, D. Milstein, *Angew. Chem. Int. Ed.* **2011**, *50*, 9948-9952; g) C. Federsel, A. Boddien, R. Jackstell, R. Jennerjahn, P. J. Dyson, R. Scopelliti, G. Laurenczy, M. Beller, *Angew. Chem. Int. Ed.* **2010**, *49*, 9777-9780; h) R. Tanaka, M. Yamashita, K. Nozaki, *J. Am. Chem. Soc.* **2009**, *131*, 14168-14169.

[4] a) X. Lu, D. Y. C. Leung, H. Wang, M. K. H. Leung, J. Xuan, *ChemElectroChem* **2014**, *1*, 836-849; b) S. Zhang, P. Kang, T. J. Meyer, *J. Am. Chem. Soc.* **2014**, *136*, 1734-1737; c) P. Kang, S. Zhang, T. J. Meyer, M. Brookhart, *Angew. Chem. Int. Ed.* **2014**, *53*, 8709-8713; d) Y. Chen, M. W. Kanan, *J. Am. Chem. Soc.* **2012**, *134*, 1986-1989.

[5] a) A. Bassegoda, C. Madden, D. W. Wakerley, E. Reisner, J. Hirst, *J. Am. Chem. Soc.* **2014**, *136*, 15473-15476; b) T. Reda, C. M. Plugge, N. J. Abram, J. Hirst, *Proc. Natl. Acad. Sci. U. S. A.* **2008**, *105*, 10654-10658.

[6] a) W. Wang, M. Niu, Y. Hou, W. Wu, Z. Liu, Q. Liu, S. Ren, K. N. Marsh, *Green Chem.* **2014**, *16*, 2614-2618; b) J. Albert, R. Wolfel, A. Bosmann, P. Wasserscheid, *Energy Environ. Sci.* **2012**, *5*, 7956-7962; c) J. Yun, F. Jin, A. Kishita, K. Tohji, H. Enomoto, *J. Phys.: Conf. Ser.* **2010**, *215*, 012126.

[7] a) Q.-L. Zhu, N. Tsumori, Q. Xu, *Chem. Sci.* **2014**, *5*, 195-199; b) Y.-L. Qin, J.-W. Wang, Y.-M. Wu, L.-M. Wang, *RSC Adv.* **2014**, *4*, 30068-30073; c) K. Jiang, K. Xu, S. Zou, W.-B. Cai, *J. Am. Chem. Soc.* **2014**, *136*, 4861-4864; d) Y. Chen, Q.-L. Zhu, N. Tsumori, Q. Xu, *J. Am. Chem. Soc.* **2014**, *137*, 106-109; e) Z.-L. Wang, J.-M. Yan, Y. Ping, H.-L. Wang, W.-T. Zheng, Q. Jiang, *Angew. Chem. Int. Ed.* **2013**, *52*, 4406-4409; f) Y.-l. Qin, J. Wang, F.-Z. Meng, L.-M. Wang, X.-B. Zhang, *Chem. Commun.* **2013**, *49*, 10028-10030; g) Q.-Y. Bi, X.-L. Du, Y.-M. Liu, Y. Cao, H.-Y. He, K.-N. Fan, *J. Am. Chem. Soc.* **2012**, *134*, 8926-8933; h) K. Tedsree, T. Li, S. Jones, C. W. A. Chan, K. M. K. Yu, P. A. J. Bagot, E. A. Marquis, G. D. W. Smith, S. C. E. Tsang, *Nat. Nanotechnol.* **2011**, *6*, 302-307.

[8] a) J. H. Barnard, C. Wang, N. G. Berry, J. Xiao, *Chem. Sci.* **2013**, *4*, 1234-1244; b) Y. Maenaka, T. Suenobu, S. Fukuzumi, *Energy Environ. Sci.* **2012**, *5*, 7360-7367; c) B. Loges, A. Boddien, H. Junge, M. Beller, *Angew. Chem. Int. Ed.* **2008**, *47*, 3962-3965; d) C. Fellay, P. J. Dyson, G. Laurenczy, *Angew. Chem. Int. Ed.* **2008**, *47*, 3966-3968; e) Y. Gao, M. C. Jennings, R. J. Puddephatt, *Organometallics* **2001**, *20*, 1882-1888.

[9] a) M. C. Neary, G. Parkin, *Chem. Sci.* **2015**, *6*, 1859-1865; b) S. Enthaler, A. Brück, A. Kammer, H. Junge, E. Irran, S. Gülak, *ChemCatChem* **2015**, *7*, 65-69; c) C. Chauvier, A. Tlili, C. Das Neves Gomes, P. Thuery, T. Cantat, *Chem. Sci.* **2015**; d) F. Bertini, I. Mellone, A. Ienco, M. Peruzzini, L. Gonsalvi, *ACS Catal.* **2015**; e) N. Scotti, R. Psaro, N. Ravasio, F. Zaccheria, *RSC Adv.* **2014**, *4*, 61514-61517; f) T. W. Myers, L. A. Berben, *Chem. Sci.* **2014**, *5*, 2771-2777; g) E. A.

Bielinski, P. O. Lagaditis, Y. Zhang, B. Q. Mercado, C. Würtele, W. H. Bernskoetter, N. Hazari, S. Schneider, *J. Am. Chem. Soc.* **2014**, *136*, 10234-10237; h) T. Zell, B. Butschke, Y. Ben-David, D. Milstein, *Chem.--Eur. J.* **2013**, *19*, 8068-8072; i) A. Boddien, D. Mellmann, F. Gärtner, R. Jackstell, H. Junge, P. J. Dyson, G. Laurenczy, R. Ludwig, M. Beller, *Science* **2011**, *333*, 1733-1736.
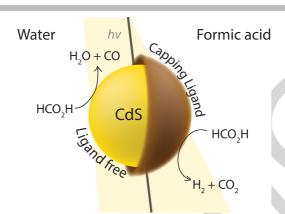
[10] a) K. Tsutsumi, N. Kashimura, K. Tabata, *Silicon* **2015**, *7*, 43-48; b) Y.-Y. Cai, X.-H. Li, Y.-N. Zhang, X. Wei, K.-X. Wang, J.-S. Chen, *Angew. Chem. Int. Ed.* **2013**, *52*, 11822-11825; c) G. Halasi, G. Schubert, F. Solymosi, *J. Phys. Chem. C* **2012**, *116*, 15396-15405.

[11] a) Z. Zheng, T. Tachikawa, T. Majima, *J. Am. Chem. Soc.* **2015**, *137*, 948-957; b) Z. Zhang, S.-W. Cao, Y. Liao, C. Xue, *Appl. Catal.: B Environ.* **2015**, *162*, 204-209.

[12] a) X. Zhang, M. Yang, J. Zhao, L. Guo, *Int. J. Hydrogen Energy* **2013**, *38*, 15985-15991; b) C. W. Lee, *Asian J. Chem.* **2013**, *25*, 5861-5864; c) Y. Li, F. He, S. Peng, D. Gao, G. Lu, S. Li, *J. Mol. Catal. A: Chem.* **2011**, *341*, 71-76; d) T. Chen, G. Wu, Z. Feng, G. Hu, W. Su, P. Ying, C. Li, *Chin. J. Catal.* **2008**, *29*, 105-107.

[13] G. Halasi, G. Schubert, F. Solymosi, *Catal. Lett.* **2012**, *142*, 218-223.

[14] B. Loges, A. Boddien, H. Junge, J. R. Noyes, W. Baumann, M. Beller, *Chem. Commun.* **2009**, 4185-4187.

[15] a) B. Zielinska, R. Janus, R. Kalenczuk, *Cent. Eur. J. Chem.* **2013**, *11*, 920-926; b) V. Lanese, D. Spasiano, R. Marotta, I. Di Somma, L. Lisi, S. Cimino, R. Andreozzi, *Int. J. Hydrogen Energy* **2013**, *38*, 9644-9654; c) A. Boddien, B. Loges, F. Gärtner, C. Torborg, K. Fumino, H. Junge, R. Ludwig, M. Beller, *J. Am. Chem. Soc.* **2010**, *132*, 8924-8934; d) S. Kakuta, T. Abe, *ACS Appl. Mater. Interfaces* **2009**, *1*, 2707-2710; e) M. Onishi, *J. Mol. Catal.* **1993**, *80*, 145-149; f) D. E. Linn Jr, R. B. King, A. D. King Jr, *J. Mol. Catal.* **1993**, *80*, 151-163.

[16] W. M. Haynes, ed., *CRC Handbook of Chemistry and Physics*, 95th ed., CRC Press/Taylor and Francis, Boca Raton, FL, **2015**.

[17] A. P. Alivisatos, *J. Phys. Chem.* **1996**, *100*, 13226-13239.

[18] M. R. Kim, D. Ma, *J. Phys. Chem. Lett.* **2014**, *6*, 85-99.

[19] a) T. Simon, N. Bouchonville, M. J. Berr, A. Vaneski, A. Adrović, D. Volbers, R. Wyrwich, M. Döblinger, A. S. Susha, A. L. Rogach, F. Jäckel, J. K. Stolarczyk, J. Feldmann, *Nat. Mater.* **2014**, *13*, 1013-1018; b) C.-B. Li, Z.-J. Li, S. Yu, G.-X. Wang, F. Wang, Q.-Y. Meng, B. Chen, K. Feng, C.-H. Tung, L.-Z. Wu, *Energy Environ. Sci.* **2013**, *6*, 2597-2602; c) L. Huang, X. Wang, J. Yang, G. Liu, J. Han, C. Li, *J. Phys. Chem. C* **2013**, *117*, 11584-11591; d) M. A. Holmes, T. K. Townsend, F. E. Osterloh, *Chem. Commun.* **2012**, *48*, 371-373; e) Z. Han, F. Qiu, R. Eisenberg, P. L. Holland, T. D. Krauss, *Science* **2012**, *338*, 1321-1324.

[20] I. Willner, Z. Goren, *J. Chem. Soc., Chem. Commun.* **1986**, 172-173.

[21] a) H. M. Yeh, S. L. Lo, M. J. Chen, H. Y. Chen, *Water Sci. Technol.* **2014**, *69*, 1676-1681; b) W. Tang, D. Jing, L. Guo, *MRS Onl. Proc. Libr.* **2011**, *1326*.

[22] X. Wang, W.-C. Peng, X.-Y. Li, *Int. J. Hydrogen Energy* **2014**, *39*, 13454-13461.

[23] a) Y. Li, L. Tang, S. Peng, Z. Li, G. Lu, *CrystEngComm* **2012**, *14*, 6974-6982; b) Y. Li, Y. Hu, S. Peng, G. Lu, S. Li, *J. Phys. Chem. C* **2009**, *113*, 9352-9358; c) S. Kambe, M. Fujii, T. Kawai, S. Kawai, F. Nakahara, *Chem. Phys. Lett.* **1984**, *109*, 105-109.

[24] Y. J. Zhang, L. Zhang, S. Li, *Int. J. Hydrogen Energy* **2010**, *35*, 438-444.

[25] A. I. Nedoluzhko, I. A. Shumilin, V. V. Nikandrov, *J. Phys. Chem.* **1996**, *100*, 17544-17550.

[26] F. Fischer, H. Tropsch, *Brennst.-Chem.* **1926**, *7*, 97-104.

[27] a) H. Konishi, K. Manabe, *Synlett* **2014**, *25*, 1971-1986; b) L. Wu, Q. Liu, R. Jackstell, M. Beller, *Angew. Chem. Int. Ed.* **2014**, *53*, 6310-6320.

[28] E. G. Graeber, D. S. Cryder, *Ind. Eng. Chem.* **1935**, *27*, 828-831.

[29] J. Aldana, N. Lavelle, Y. Wang, X. Peng, *J. Am. Chem. Soc.* **2005**, *127*, 2496-2504.

[30] W. W. Yu, L. Qu, W. Guo, X. Peng, *Chem. Mater.* **2003**, *15*, 2854-2860.

[31] a) C. Gimbert-Suriñach, J. Albero, T. Stoll, J. Fortage, M.-N. Collomb, A. Deronzier, E. Palomares, A. Llobet, *J. Am. Chem. Soc.* **2014**, *136*, 7655-7661; b) A. Das, Z. Han, M. G. Haghighi, R. Eisenberg, *Proc. Natl. Acad. Sci. U. S. A.* **2013**, *110*, 16716-16723.

[32] C. Jung, C. M. Sánchez-Sánchez, C.-L. Lin, J. Rodríguez-López, A. J. Bard, *Anal. Chem.* **2009**, *81*, 7003-7008.

[33] T. J. Kemp, W. A. Waters, *Proc. R. Soc. A* **1963**, *274*, 480-499.

[34] A. S. Feiner, A. J. McEvoy, N. Vlachopoulos, M. Grätzel, *Berichte der Bunsengesellschaft für physikalische Chemie* **1987**, *91*, 399-402.

[35] E. L. Rosen, R. Buonsanti, A. Llordes, A. M. Sawvel, D. J. Milliron, B. A. Helms, *Angew. Chem. Int. Ed.* **2012**, *51*, 684-689.

[36] J. Liu, X. Yang, K. Wang, D. Wang, P. Zhang, *Chem. Commun.* **2009**, 6080-6082.

[37] a) K. L. Miller, J. L. Falconer, J. W. Medlin, *J. Catal.* **2011**, *278*, 321-328; b) K. L. Miller, C. W. Lee, J. L. Falconer, J. W. Medlin, *J. Catal.* **2010**, *275*, 294-299.

[38] J. Cho, S. Lee, J. Han, S. P. Yoon, S. W. Nam, S. H. Choi, K.-Y. Lee, H. C. Ham, *J. Phys. Chem. C* **2014**, *118*, 22553-22560.

[39] R. Zhang, H. Liu, B. Wang, L. Ling, *J. Phys. Chem. C* **2012**, *116*, 22266-22280.

[40] P. Mars, J. J. F. Scholten, P. Zwietering, in *Adv. Catal., Vol. Volume 14* (Eds.: H. P. D.D. Eley, B. W. Paul), Academic Press, **1963**, pp. 35-113.

Entry for the Table of Contents

COMMUNICATION

Selective photocatalytic conversion of formic acid to either H_2 or CO is achieved in the presence of inexpensive CdS nanocrystals under visible-light irradiation. Product selectivity is controlled by the solvent and particle capping ligand and high photoactivity is sustained for several days under ambient conditions.

Moritz F. Kuehnel,[‡] David W. Wakerley,[‡] Katherine L. Orchard, and Erwin Reisner*

Page No. – Page No.

Photocatalytic Formic Acid Conversion on CdS Nanocrystals with Controllable Selectivity for H_2 or CO